Published in final edited form as:
J Thorac Cardiovasc Surg. 2011 February ; 141(2): 345–353. doi:10.1016/j.jtcvs.2010.10.015.

Effects of Different Annuloplasty Ring Types on Mitral Leaflet Tenting Area During Acute Myocardial Ischemia

Wolfgang Bothe, MD[1], **John-Peder Escobar Kvitting, MD PhD**[1], **Elizabeth H. Stephens, PhD**[2], **Julia C. Swanson, MD**[1], **David H. Liang, MD PhD**[3], **Neil B. Ingels Jr., PhD**[1,4], and **D. Craig Miller, MD**[1]

[1]Department of Cardiothoracic Surgery, Stanford University School of Medicine, Stanford, CA

[2]Department of Bioengineering, Rice University, Houston, TX

[3]Division of Cardiovascular Medicine, Stanford University School of Medicine, Stanford, CA

[4]Laboratory of Cardiovascular Physiology and Biophysics, Research Institute of the Palo Alto Medical Foundation, Palo Alto, CA

Abstract

OBJECTIVE—To quantify effects of different annuloplasty rings on mitral leaflet septal-lateral (S-L) tenting areas (TAs) during acute myocardial ischemia.

METHODS—Radiopaque markers were implanted in 30 sheep: two to the S-L aspects of the mitral annulus; four and two along the central S-L meridian of anterior and posterior mitral leaflet (AML, PML), respectively. Ten true-sized Carpentier-Edwards Physio (PHYSIO), Edwards IMR-ETLogix (ETL) and GeoForm (GEO) annuloplasty rings were inserted in a releasable fashion. Marker coordinates were obtained using biplane videofluoroscopy with ring inserted, at baseline (RING_BL), and after 90s of LCx occlusion (RING_ISCH). After ring release, another dataset was acquired before (No_Ring_BL) and after LCx occlusion (No_Ring_ISCH). AML and PML 3-D TAs were computed at mid-systole from sums of marker triangles with the midpoint between the annular markers being the vertex for all triangles.

RESULTS—Compared to No_Ring_BL, MR grades and all TAs significantly increased with No_Ring_ISCH. Relative to No_Ring_ISCH: 1.) All rings significantly prevented MR and reduced all TAs; 2.) ETL and GEO reduced PML, but not AML TA to a significantly greater extent than PHYSIO; and, 3.) ETL and GEO affected TAs similarly.

CONCLUSIONS—In response to acute LV ischemia, disease specific FMR/IMR rings (ETL, GEO) more effectively reduced PML, but not AML TA compared to true-sized physiological rings (PHYSIO). Despite its radical 3-D shape and greater amount of mitral annular S-L downsizing, GEO did not reduce TAs more than ETL, suggesting that further reduction in TAs may not be effectively achieved using annular size reduction.

Address for correspondence: D. Craig Miller, M.D., Department of Cardiothoracic Surgery, Falk Cardiovascular Research Center, Stanford University School of Medicine, Stanford, California 94305-5247, 001.650.725.3826 FAX 001.650.725.3846 dcm@stanford.edu.

Presented at the C. Walton Lillehei Resident Forum Session at the 90th Annual Meeting of the American Association for Thoracic Surgery, Toronto, Canada, May 1–5, 2010

INTRODUCTION

Functional/ischemic mitral regurgitation (FMR/IMR) is associated with left ventricular (LV) dilatation and papillary muscle displacement [1], which leads, via annular dilation and chordal tethering, to complex three-dimensional (3-D) alterations of the mitral valve geometry. While the central anterior leaflet belly displaces towards the apex ("leaflet tenting") [2–7], the edges of anterior and posterior leaflet may displace apically, prolapse or both [8].

Various parameters are available to describe and quantify changes in leaflet geometry during FMR/IMR [3–7,9,10]. One of the most common parameters to quantify the degree of FMR/IMR includes the assessment of the mitral leaflet tenting area, which describes the area between mitral annulus and both leaflets in a central, longitudinal, septal-lateral mitral-annular cross-section during systole. The amount of tenting area strongly correlates with the severity of FMR/IMR [6] and may be a predictive factor for recurrent mitral regurgitation (MR) in patients with FMR/IMR undergoing mitral valve repair [11].

Although the results of surgical valve repair for FMR/IMR have significantly improved recently with rigid, undersized ring annuloplasty having become the current procedure of choice [3], outcomes continue to be suboptimal with current MR recurrence rates as high as ~15% (mitral regurgitation grade 2+ or higher) 3–5 years post-operatively [3,12]).

The primary reason for recurrent FMR/IMR is progressive LV dilatation leading to increased leaflet tethering and, ultimately, leaflet malcoaptation and recurrent regurgitation [13]. To account for the underlying pathophysiology, disease specific annuloplasty rings (Edwards GeoForm, IMR-ETLogix) have been designed that aim to treat these typical subvalvular alterations on an annular level.

The key feature of these rings includes a disproportionate reduction of the mitral annular septal-lateral dimension. We recently demonstrated that, compared to a Carpentier Edwards Physio, the approximate amount of septal-lateral reduction includes 10% and 18% for the Edwards IMR ETLogix as well as 25% and 26% for the Edwards GeoForm *in vitro* [14] and in the normal beating ovine heart [15], respectively. To date, two clinical studies exist that report the effects of the IMR ETlogix on tenting area [5,16] and one that shows tenting volume after implantation of the GeoForm [17]. Daimon et al. [5] and Filsoufi et al. [16] report a reduction in tenting area by ~50% and ~60%, respectively, after the implantation of an IMR ETlogix in 59 and 40 IMR patients, respectively, while Armen et al. demonstrate a reduction in tenting volume of ~75% after implantation of the GeoForm in a series of 7 patients with IMR [17]. However, to date no study exists that compares the effects of the different ring types on mitral valve tenting area in a homogenous patient population.

Our goal was therefore to quantify the effects of physiological (Carpentier-Edwards Physio) and IMR specific (Edwards GeoForm and IMR-ETLogix) annuloplasty rings on changes in mitral valve tenting area during acute myocardial ischemia in an ovine model using 4-D radiopaque marker tracking and a releasable ring insertion technique.

MATERIAL AND METHODS

Surgical preparation

36 adult, Dorsett-hybrid, male sheep (49±4kg) were premedicated with ketamine (25mg/kg intramuscularly), anesthetized with sodium thiopental (6.8mg/kg intravenously), intubated and mechanically ventilated with inhalational isoflurane (1.0–2.5%). All animals received humane care in compliance with the *Principles of Laboratory Animal Care* formulated by

the National Society of Medical Research and the *Guide for Care and Use of Laboratory Animals* prepared by the National Academy of Sciences and published by the National Institute of Health (DHEW NIHG publication 85-23, revised 1985). This study was approved by the Stanford Medical Center Laboratory Research Animal Review committee and conducted according to Stanford University policy.

Through a left thoracotomy, 13 radiopaque markers were implanted to silhouette the LV at the cross-section points of four equally spaced longitudinal and three equatorial meridians as described earlier [14]. Using cardiopulmonary bypass and cardioplegic arrest, 8 radiopaque markers were implanted as follows: two markers were sewn to the septal-lateral (S-L) aspect (#22 and 18, Figure 1A) and two to the anterior and posterior mitral annular commissures (#ACOM and PCOM, respectively). Four and two markers were sutured along the S-L meridian of the anterior and posterior mitral leaflets (AML (#A1–A4, Figure 1A) and PML (#P1 and P2, Figure 1A)), respectively (single tantalum loops, 0.6 mm ID, 1.1 mm OD, 3.2 mg each). In order to allow each animal to serve as its own Control, either a Carpentier-Edwards Physio (PHYSIO), an Edwards IMR ETLogix (ETL) or an Edwards GeoForm (GEO) annuloplasty ring (Edwards Lifesciences, Irvine, CA) was implanted in a releasable fashion as previously described [19].

In brief, the mid part of eight double-armed polyester sutures were placed evenly spaced through the annuloplasty ring before the operation using a French eye needle and the resulting loops were locked with polypropylene sutures (“locking sutures”). Additionally, two drawstring sutures were attached to the ring. During the operation, the ends of the eight polyester sutures were sewn equidistantly in a perpendicular direction from the ventricular to the atrial side through the mitral annulus. The annuloplasty ring was secured to the mitral annulus by tying these sutures. The “locking sutures” and the drawstrings were exteriorized, and the left atrium was closed. Animals were randomly assigned to receive either Edwards Cosgrove, Saint Jude Medical RSAR, PHYSIO or GEO. Since this manuscript focuses on the effects of IMR specific annuloplasty rings, data from Cosgrove and RSAR are not reported. After the implantation of these four ring types the IMR ETlogix was added. Consequently, animals receiving this ring type were not randomized. All annuloplasty rings were “true-sized” by assessing the height and entire anterior mitral leaflet area. As all animals had similarly sized leaflets, all received size 28 rings. The left circumflex artery (LCx) was then encircled with a vessel loop immediately distal to the first OM branch. The sheep, while intubated and anesthetized, were then transferred with the chest open to the experimental catheterization laboratory.

Data acquisition

Six out of the 36 animals could not be used for data acquisition due to complications related to the surgical procedure and the induction of ischemia. Videofluoroscopic images (60 frames/sec) of all radiopaque markers were acquired using biplane videofluoroscopy (Philips Medical Systems, North America, Pleasanton, CA, USA). Figure 1C shows the experimental protocol schematically. First, images were acquired with the ring inserted under baseline (BL) conditions (PHYSIO:Ring_BL, ETL:Ring_BL, GEO:Ring_BL). Acute LV ischemia was then induced by tightening the LCx loop for 90 sec, and another dataset under ischemic conditions (ISCH) was obtained (PHYSIO:Ring_ISCH, ETL:Ring_ISCH, GEO:Ring_ISCH). The locking sutures were then withdrawn and the ring was lifted away from the mitral annulus into the left atrium using the drawstrings. After hemodynamic values returned to baseline, a third data acquisition was performed and images were acquired under baseline conditions with the ring released (PHYSIO:No_Ring_BL, ETL:No_Ring_BL, GEO:No_Ring_BL). As described previously, this baseline data without ring implanted is comparable to baseline data from studies where no ischemia was induced and no ring was implanted [19]. After the acquisition of baseline data with no ring

implanted, 90s of LCx ischemia were induced (PHYSIO:No_Ring_ISCH, ETL:No_Ring_ISCH, GEO:No_Ring_ISCH). In order to determine whether 90s of LCx occlusion would be appropriate to assess differences between ring types, LV geometry and papillary muscle displacement vectors during this ischemia period were analyzed and found to be similar to historic studies from our lab where longer periods of acute ischemia were induced.

Marker coordinates from three consecutive sinus rhythm beats from each of the biplane views were then digitized and merged to yield the time-resolved 3-D coordinates of each marker centroid in each frame using semi-automated image processing and digitization software [20,21]. ECG and analog left ventricular pressure (LVP) were recorded in real-time on the video images. The amount of mitral regurgitation after each data acquisition run was independently graded by an expert echocardiographer (D.H.L.) on the basis of color Doppler regurgitant jet extent and width [22] and categorized as none (0), mild (+1), moderate (+2), moderate-to-severe (+3), or severe (+4).

Data analysis

For each beat, end-diastole (ED) was defined as the videofluoroscopic frame containing the peak of the R-wave on the ECG and end-systole (ES) as the frame preceding maximum peak rate fall of the left ventricular pressure (−dP/dt). Distances between anterior and posterior leaflet edge ($d_{AML/PML}$) were computed throughout the cardiac cycle as distances between markers #A_1 and #B_1 (Figure 1A). Closure Frame 1 was defined as the frame when $d_{AML/PML}$ fell to a stable minimum value with valve closure immediately after ED. Closure Frame 2 was defined as the frame when $d_{AML/PML}$ just began to increase with valve opening after IVR. Time of mid-systole was defined as: ((Closure Frame 2 – Closure Frame 1)/2) + Closure Frame 1.

Hemodynamics

Instantaneous LV volume was computed from the epicardial LV markers using a space-filling multiple tetrahedral volume method [20]. Hemodynamic data were calculated from marker derived instantaneous LV volumes and analog LV pressures [23].

Mitral valve tenting area

tenting area was computed at mid-systole from sums of marker triangles with the mid point between the saddle horn (#22, Figure 1A) and mid-lateral posterior annular marker (#18, Figure 1A) being the vertex for all triangles, as illustrated in Figure 1B. Markers #22, A_1, A_2, A_3, A_4, 18, P_1 and P_2 were the base of the triangles for the total tenting area. In order to obtain insight into ring effects on tenting area across AML and PML, total tenting area was divided into AML and PML tenting area. Markers #22, A_1, A_2, A_3 and A_4 were the base of the triangles for AML and #18, P_1 and P_2 were the base of the triangles for the PML tenting areas (Figure 1B). Percent changes in tenting areas were calculated between No_Ring_ISCH *vs.* Ring_ISCH as 100*(tenting area Ring_ISCH - tenting area No_Ring_ISCH)/tenting area No_Ring_ISCH and between Ring_BL *vs.* Ring_ISCH as 100*(tenting area Ring_ISCH - tenting area No_Ring_BL)/tenting area No_Ring_BL.

Mitral annular dimensions

The septal-lateral mitral annular dimension was calculated as the distance in 3-D space between the saddle horn and mid-lateral posterior annular markers (#22 and 18, respectively) and the commissure-commissure MA dimension as the distance between the anterior and posterior commissural annular markers (#ACOM and PCOM) at mid-systole.

Statistical analysis

Data are reported as mean ±1 SD unless otherwise stated. Continuous data were compared within each group using 2-tailed Student's *t*-test for paired observations with *post hoc* Bonferroni correction (significance level set at p<.005). Ring types were contrasted by comparing absolute changes between the individual states (No_Ring_BL *vs.* No_Ring_ISCH, Ring_BL *vs.* Ring_ISCH, No_Ring_ISCH *vs.* Ring_ISCH) between the three groups (PHYSIO, ETL, GEO) using analysis of variance (ANOVA) with *post hoc* Holm-Sidak correction (Sigmastat 3.5, Systat Software, Inc, San Jose, CA, USA) with a p-value < 0.05 considered to be statistically significant.

RESULTS

Hemodynamics

Table 1 summarizes the hemodynamic changes and mitral annular dimensions measured under baseline conditions (No_Ring_BL, Ring_BL) and during ischemia (No_Ring_ISCH, Ring_ISCH), which were consistent with acute ischemia as reflected by increased LVEDP, decreased maximum LVP and dP/dt absolute values. Heart rate did not change during ischemia. MR grade was significantly greater during ischemia without ring implantation (No_Ring_ISCH) in all groups compared to baseline (No_Ring_BL); furthermore, all three rings effectively prevented MR during acute LV ischemia.

Mitral valve tenting areas

Septal-lateral tenting areas—Without an annuloplasty ring implanted, all tenting areas (total, AML and PML tenting area) increased significantly during ischemia (No_Ring_BL *vs.* No_Ring_ISCH, all p<.05, Figure 2).

Ring implantation significantly reduced all tenting areas (total, AML, and PML tenting area) during LV ischemia (No_Ring_ISCH *vs.* Ring_ISCH, all p<.05, Figure 3A-C). Figure 4A shows the relative changes in tenting area between the individual states. During ischemia, ETL and GEO reduced total and PML tenting area (No_Ring_ISCH *vs.* Ring_ISCH: ETL vs. PHYSIO, p<.05 and GEO vs. PHYSIO, p<.05, Figure 4A), but not AML tenting area compared to PHYSIO (No_Ring_ISCH *vs.* Ring_ISCH: ETL vs. PHYSIO, n.s. and GEO vs. PHYSIO, n.s., Figure 4A). The relative amount of PML tenting area reduction during ischemia was approximately two times greater with ETL and GEO compared to PHYSIO (No_Ring_ISCH *vs.* Ring_ISCH, −23.7±10.1% and −22.1±7.1% *vs.* −11.0±7.5%, respectively, both p<.05, Figure 4A).

Figure 3D-F shows the changes in tenting areas with the respective rings implanted (Ring BL *vs.* Ring ISCH). Despite the presence of an annuloplasty ring, the induction of ischemia resulted in an increase of PML tenting area in the PHYSIO group (Ring_BL *vs.* Ring_ISCH, p<.05, Figure 3D) and of total and AML tenting area in the GEO group (Ring_BL *vs.* Ring_ISCH, both p<.05, Figure 3F).

Mitral annular dimensions

Table 1 shows the mitral annular dimensions for all groups. With no ring implanted, mitral annular S-L and C-C dimensions increased in all three groups during ischemia (No_Ring_BL *vs.* No_Ring_ISCH, all p<.005). Relative to ischemia without ring, all rings significantly reduced both mitral annular S-L and C-C diameter (No_Ring_ISCH *vs.* Ring_ISCH, all p<.005). Figure 4B shows the relative changes in mitral annular dimensions. GEO provided the greatest amount of mitral annular S-L reduction, followed by ETL and PHYSIO (GEO:−30±4% *vs.* ETL:−21±4%, p<.05, and ETL:−21±4% *vs.* PHYSIO:−11±8%, p<.05). In contrast, PHYSIO and ETL provided a greater amount of mitral annular **C-C**

reduction than GEO (−17±4% and −19±3% *vs.* −8±5%, respectively, both p<.05). After any of the 3 types of rings was implanted, no relevant changes in mitral annular dimensions during ischemia were observed (Ring_BL *vs.* Ring_ISCH).

DISCUSSION

The principal findings of this study were: 1.) Acute posterolateral LV ischemia increased all tenting areas, *i.e.*, total, AML and PML tenting area; 2.) All three ring types reduced ischemia-induced increases in all 3 tenting areas; however, ETL and GEO reduced total and PML, but not AML tenting area to a greater extent than did PHYSIO; 3.) Although GEO reduced the mitral annular S-L dimension to a greater extent than ETL, the effects of ETL and GEO on AML and PML tenting areas during ischemia were similar.

Effect of acute posterolateral LV ischemia on tenting areas: No_Ring_BL *vs.* No_Ring_ISCH

Without the presence of an annuloplasty ring all measured tenting areas (total, AML and PML tenting area) increased with acute localized posterolateral LV wall ischemia. Watanabe *et al.* measured AML and PML tenting heights in twelve patients with chronic IMR using real time 3-D echocardiography and found that maximum tenting occurred in the AML and never in the PML [24]. In contrast, we found that the absolute increases in AML and PML tenting areas with no ring implanted were identical (No_Ring_BL *vs.* No_Ring_ISCH, AML: +0.09±0.07cm^2, PML: +0.09±0.06cm^2). This discordance in findings could be explained by several factors, including the length of ischemia (acute *vs.* chronic), the site of LV wall ischemia (localized posterolateral *vs.* multi-segmental ischemia), different species, and/or the differences in imaging modalities used. Regardless of these differences, our data indicate that PML tethering plays an equally important role in the pathophysiology of IMR under these acute experimental conditions. This hypothesis is supported by Magne *et al.* who found that the degree of preoperative PML tethering is a predictive factor for recurrent MR in patients with IMR undergoing ring annuloplasty [7].

Effect of annuloplasty ring implantation on tenting areas during acute myocardial ischemia: No_Ring_ISCH *vs.* Ring_ISCH

To date, neither clinical nor experimental *in vivo* studies exist comparing the effects of conventional annuloplasty rings to disease-specific FMR/IMR rings on mitral valve geometry or mitral annular dimensions during myocardial ischemia. In this *in vivo* experimental ovine preparation, the relative amount of mitral annular S-L reduction during acute myocardial ischemia after ring implantation (No_Ring_ISCH *vs.* Ring_ISCH, Figure 4A) was smallest for PHYSIO (−15±4%), greater for ETL (−21±4%), and largest for GEO (−30±4%). These amounts of mitral annular S-L reduction are slightly less compared to those reported previously in *in vitro* measurements and [14] beating ovine, non-ischemic hearts [15]. However, the reduction in tenting area compared to pre-implantation values was considerably smaller than those reported in clinical studies, where the approximate decrease in tenting area included 50–60% after IMR Etlogix ring implantation [5, 16] and 75% in tenting volume after GeoForm implantation [10]. These observed discrepancies are most probably due a greater tethering of the mitral valve before ring implantation in patients with chronic IMR compared to sheep valves during acute IMR. It is reasonable to assume that the effects of ring implantation on tenting area reduction are therefore considerably greater in patients.

Effect of ischemia on tenting areas with annuloplasty rings inserted: Ring_BL *vs.* Ring_ISCH

Another interesting observation was that tenting areas may be affected by regional ischemia despite the presence of an annuloplasty ring and the absence of MR (increases in total and AML tenting area with GEO and in PML tenting area with PHYSIO, Figure 3). These findings demonstrate that annuloplasty rings, although efficient in restoring valvular competence, cannot prevent ischemia-induced alterations in mitral subvalvular geometry. While it remains speculative whether abnormal tenting areas play a role in the mechanism of recurrent MR postoperatively, it is reasonable to assume that these changes may adversely affect leaflet stress distribution patterns and, *pari passu*, potentially jeopardize long-term repair durability.

Clinical inferences

With respect to tenting area, we found that all three ring types decreased all tenting areas. Interestingly, the amount of mitral annular S-L reduction was not directly proportional to the decrease in tenting areas observed. While PHYSIO decreased total and PML tenting area to the least extent (No Ring ISCH *vs.* Ring ISCH, Figure 4A), ETL and GEO provided a greater – and similar - amount of reduction in total, AML and PML tenting area (Figure 4A). These results indicate that despite more mitral annular S-L downsizing, its dog-bone shape, and elevation of the mid-posterior ring segment, GEO did not provide additional improvement in terms of reducing tenting areas compared to ETL. Hypothetically, GEO's more radical mitral annular septal-lateral downsizing could induce leaflet displacements which may prevent further reduction of tenting areas on an annular level. It is conjectured that the addition of a subvalvular adjunctive procedure, *e.g.* as proposed by Kron *et al.* or Langer *et al.*, may provide additional benefit in terms of tenting area reduction [25, 26]. Furthermore, compared to PHYSIO, the ETL and GEO rings were more effective in reducing PML, but not AML tenting area. These findings indicate that main effect of annuloplasty rings is to pull the PML towards the AML, which - at least in this acute model - suggests that IMR annuloplasty rings should be designed to target the posterior muscular mitral annular sector instead of the fibrous anterior portion of the mitral annulus.

Limitations

Caution is certainly necessary in extrapolating these acute experimental findings to patients. First, differences between ovine and human mitral valve anatomy exist. Walmsley [27] e.g. reported that the central zone of the anterior mitral leaflet is more rigid in sheep hearts than in human hearts. Such rigidity might attenuate alterations in tenting area compared to patients, although we assume it is a minor contributor since ovine leaflets are nonetheless very flexible. Furthermore, from our own experience the position of the papillary muscles relative to the leaflets may be slightly different in sheep *vs.* humans and, thus, could impair the extrapolation of our findings to patients. Second, the pathological perturbations of this acute ischemic experimental preparation undoubtedly differ from those in patients with chronic FMR/IMR, even though previous studies from our laboratory have shown that papillary muscle displacement differs only slightly between acute and chronic ovine ischemic models: For example, Lai *et al.* [28] in an ovine model of acute IMR found antero-apical and postero-basal displacement of the anterior and posterior papillary muscle tips, respectively whereas Tibayan *et al.* [29] induced chronic IMR in sheep and noted postero-lateral and postero-lateral plus basal displacement of the anterior and posterior papillary muscle tips, respectively. Presumably these differences in 3-D papillary muscle behavior between acute and chronic ischemia affect 3-D leaflet geometry: Ryan *et al.*, found that the tenting sites with ischemic MR were most prominent between the two commissures during acute, but more pronounced towards the anterior commissure during chronic IMR [9]. Future studies in a chronic experimental setting or in patients with chronic IMR focused on

the effects of rings are needed. A third limitation is that downsized ring annuloplasty is the procedure of choice when using Physio rings in patients with IMR/FMR [3,30,31], but in our study disease specific IMR ETLogix and GeoForm rings were compared to true sized Physio rings. The benefit of disease specific ring designs compared to a downsized Physio ring can therefore not be assessed and no recommendation can be made with respect to the use of a Physio ring for the treatment of IMR. Fourth, our experimental approach tracks distinct anatomic landmarks in all three dimensions and, thus, includes displacements of the respective structures in any direction in 3-D space. Consequently, our results may differ from tenting area measurements obtained from clinical imaging techniques where only one 2-D longitudinal cross-sectional view is obtained. Lastly, the quantification of tenting areas and the separation into AML and PML tenting area after valve repair using current clinical imaging modalities may be difficult due to artifacts resulting from ring implantation.

In conclusion, disease specific FMR/IMR rings (ETL, GEO) reduced total tenting area to a greater extent in response to acute LV ischemia than did true-sized PHYSIO rings. This reduction was predominantly due to a greater decrease in PML tenting area, suggesting that IMR annuloplasty rings should be designed to target the posterior muscular mitral annular sector instead of the fibrous anterior portion of the mitral annulus. Furthermore, despite its radical 3-D shape and greater amount of mitral annular S-L downsizing, GEO did not reduce tenting areas more than ETL. We therefore hypothesize that radical septal-lateral downsizing could induce leaflet displacements that may prevent a further reduction of tenting areas on an annular level. Clinical studies are needed to determine whether these findings translate to patients.

Acknowledgments

We thank Paul Chang, Maggie Brophy, George T. Daughters III, Sigurd Hartnett, Saideh Fahramand, Lauren R. Davis, Eleazar Briones and Kathy Vo for expert technical assistance.

Supported by grants HL-29589 and HL-67025 from the National Heart, Lung and Blood Institute.

Dr. Bothe was supported by the Deutsche Herzstiftung, Frankfurt, Germany.

Dr. Kvitting was funded by U.S. - Norway Fulbright Foundation, Swedish Heart-Lung Foundation and the Swedish Society for Medical Research

Dr. Swanson was funded by Western States Affiliate American Heart Association Postdoctoral Fellowship

Dr Miller is a consultant for Medtronic Heart Valve Division, Inc. and St. Jude Medical; he also is a non-compensated member of the Edwards PARTNER U.S. Pivotal Trial Executive Committee.

ABBREVIATIONS AND ACRONYMS

IMR/FMR	Ischemic/functional mitral regurgitation
AML	Anterior Mitral Leaflet
PML	Posterior Mitral Leaflet
ETL	Edwards IMR ETLogix annuloplasty ring
GEO	Edwards GeoForm annuloplasty ring
LCx	Left circumflex artery
LVP	Left ventricular pressure (mmHg)
LV	Left ventricle

S-L	Septal-lateral
C-C	Commissure-commissure

REFERENCES

1. Kwan J, Shiota T, Agler DA, Popovic ZB, Qin JX, Gillinov MA, et al. Geometric differences of the mitral apparatus between ischemic and dilated cardiomyopathy with significant mitral regurgitation: real-time three-dimensional echocardiography study. Circulation 2003;107:1135–1140. [PubMed: 12615791]
2. Gelsomino S, Lorusso R, De Cicco G, Capecchi I, Rostagno C, Caciolli S, et al. Five-year echocardiographic results of combined undersized mitral ring annuloplasty and coronary artery bypass grafting for chronic ischaemic mitral regurgitation. Eur Heart J 2008;29:231–240. [PubMed: 17989079]
3. Braun J, van de Veire NR, Klautz RJ, Versteegh MI, Holman ER, Westenberg JJ, et al. Restrictive mitral annuloplasty cures ischemic mitral regurgitation and heart failure. Ann Thorac Surg 2008;85:430–436. discussion 436-7. [PubMed: 18222238]
4. Watanabe N, Ogasawara Y, Yamaura Y, Yamamoto K, Wada N, Kawamoto T, et al. Geometric differences of the mitral valve tenting between anterior and inferior myocardial infarction with significant ischemic mitral regurgitation: quantitation by novel software system with transthoracic real-time three-dimensional echocardiography. J Am Soc Echocardiogr 2006;19:71–75. [PubMed: 16423672]
5. Daimon M, Fukuda S, Adams DH, McCarthy PM, Gillinov AM, Carpentier A, et al. Mitral valve repair with Carpentier-McCarthy-Adams IMR ETlogix annuloplasty ring for ischemic mitral regurgitation: early echocardiographic results from a multi-center study. Circulation 2006;114:I588–I593. [PubMed: 16820643]
6. Song JM, Qin JX, Kongsaerepong V, Shiota M, Agler DA, Smedira NG, et al. Determinants of ischemic mitral regurgitation in patients with chronic anterior wall myocardial infarction: a real time three-dimensional echocardiography study. Echocardiography 2006;23:650–657. [PubMed: 16970716]
7. Magne J, Pibarot P, Dagenais F, Hachicha Z, Dumesnil JG, Senechal M. Preoperative posterior leaflet angle accurately predicts outcome after restrictive mitral valve annuloplasty for ischemic mitral regurgitation. Circulation 2007;115:782–791. [PubMed: 17283262]
8. Bothe W, Nguyen TC, Ennis DB, Itoh A, Carlhall CJ, Lai DT, et al. Effects of acute ischemic mitral regurgitation on three-dimensional mitral leaflet edge geometry. Eur J Cardiothorac Surg 2008;33:191–197. [PubMed: 18321461]
9. Ryan L, Jackson B, Parish L, Sakamoto H, Plappert T, Sutton MS, et al. Quantification and localization of mitral valve tenting in ischemic mitral regurgitation using real-time three-dimensional echocardiography. Eur J Cardiothorac Surg 2007;31:839–844. [PubMed: 17329114]
10. Armen TA, Vandse R, Crestanello JA, Raman SV, Bickle KM, Nathan NS. Mechanisms of valve competency after mitral valve annuloplasty for ischaemic mitral regurgitation using the Geoform ring: insights from three-dimensional echocardiography. Eur J Echocardiogr 2009;10:74–81. [PubMed: 18490271]
11. Lee AP, Acker M, Kubo SH, Bolling SF, Park SW, Bruce CJ, et al. Mechanisms of recurrent functional mitral regurgitation after mitral valve repair in nonischemic dilated cardiomyopathy: importance of distal anterior leaflet tethering. Circulation 2009;119:2606–2614. [PubMed: 19414639]
12. Pocar M, Passolunghi D, Moneta A, Di Mauro A, Bregasi A, Mattioli R, et al. Baseline left ventricular function and surgical annular stiffening to predict outcome and reverse left ventricular remodeling after undersized annuloplasty for intermediate-degree ischemic mitral regurgitation. J Thorac Cardiovasc Surg. 2009
13. Matsunaga A, Tahta SA, Duran CM. Failure of reduction annuloplasty for functional ischemic mitral regurgitation. J Heart Valve Dis 2004;13:390–397. discussion 397-8. [PubMed: 15222285]

14. Bothe W, Swanson JC, Ingels NB, Miller DC. How much septal-lateral mitral annular reduction do you get with new ischemic/functional mitral regurgitation annuloplasty rings? J Thorac Cardiovasc Surg. 2010 doi:10.1016/j.jtcvs.2009.10.033.
15. Bothe W, Kvitting JP, Swanson JC, Hartnett S, Ingels NB, Miller DC. Effects of Different Annuloplasty Rings on Anterior Mitral Leaflet Dimensions. J Thorac Cardiovasc Surg 2010;139:1114–1122. [PubMed: 20412950]
16. Filsoufi F, Castillo JG, Rahmanian PB, Carpentier A, Adams DH. Remodeling annuloplasty using a prosthetic ring designed for correcting type-IIIb ischemic mitral regurgitation. Rev Esp Cardiol 2007;60:1151–1158. [PubMed: 17996175]
17. Armen TA, Vandse R, Crestanello JA, Raman SV, Bickle KM, Nathan NS. Mechanisms of valve competency after mitral valve annuloplasty for ischaemic mitral regurgitation using the Geoform ring: insights from three-dimensional echocardiography. Eur J Echocardiogr. 2008
18. Timek TA, Dagum P, Lai DT, Liang D, Daughters GT, Tibayan F, et al. Tachycardia-induced cardiomyopathy in the ovine heart: mitral annular dynamic three-dimensional geometry. J Thorac Cardiovasc Surg 2003;125:315–324. [PubMed: 12579100]
19. Bothe W, Chang PA, Swanson JC, Itoh A, Arata K, Ingels NB, et al. Releasable annuloplasty ring insertion--a novel experimental implantation model. Eur J Cardiothorac Surg 2009;36:830–832. [PubMed: 19646892]
20. Niczyporuk MA, Miller DC. Automatic tracking and digitization of multiple radiopaque myocardial markers. Comput Biomed Res 1991;24:129–142. [PubMed: 2036779]
21. Daughters G, Sanders W, Miller D, Schwarzkopf A, Mead C, Ingels N. A comparison of two analytical systems for 3-D reconstruction from biplane videoradiograms. IEEE Computers in Cardiology 1989;15:79–82.
22. Helmcke F, Nanda NC, Hsiung MC, Soto B, Adey CK, Goyal RG, et al. Color Doppler assessment of mitral regurgitation with orthogonal planes. Circulation 1987;75:175–183. [PubMed: 3791603]
23. Glasson JR, Komeda M, Daughters GT 2nd, Bolger AF, Ingels NB Jr. Miller DC. Loss of three-dimensional canine mitral annular systolic contraction with reduced left ventricular volumes. Circulation 1996;94:II152–II158. [PubMed: 8901737]
24. Watanabe N, Ogasawara Y, Yamaura Y, Kawamoto T, Toyota E, Akasaka T, et al. Quantitation of mitral valve tenting in ischemic mitral regurgitation by transthoracic real-time three-dimensional echocardiography. J Am Coll Cardiol 2005;45:763–769. [PubMed: 15734623]
25. Kron IL, Green GR, Cope JT. Surgical relocation of the posterior papillary muscle in chronic ischemic mitral regurgitation. Ann Thorac Surg 2002;74:600–601. [PubMed: 12173864]
26. Langer F, Kunihara T, Hell K, Schramm R, Schmidt KI, Aicher D, et al. RING+STRING: Successful repair technique for ischemic mitral regurgitation with severe leaflet tethering. Circulation 2009;120:S85–S91. [PubMed: 19752391]
27. Walmsley R. Anatomy of human mitral valve in adult cadaver and comparative anatomy of the valve. Br Heart J 1978;40:351–366. [PubMed: 565642]
28. Lai DT, Timek TA, Tibayan FA, Green GR, Daughters GT, Liang D, et al. The effects of mitral annuloplasty rings on mitral valve complex 3-D geometry during acute left ventricular ischemia. Eur J Cardiothorac Surg 2002;22:808–816. [PubMed: 12414050]
29. Tibayan FA, Rodriguez F, Zasio MK, Bailey L, Liang D, Daughters GT, et al. Geometric distortions of the mitral valvular-ventricular complex in chronic ischemic mitral regurgitation. Circulation 2003;108 Suppl 1:II116–II121. [PubMed: 12970219]
30. Spoor MT, Geltz A, Bolling SF. Flexible versus nonflexible mitral valve rings for congestive heart failure: differential durability of repair. Circulation 2006;114:I67–I71. [PubMed: 16820648]
31. Williams ML, Daneshmand MA, Jollis JG, Horton JR, Shaw LK, Swaminathan M, et al. Mitral gradients and frequency of recurrence of mitral regurgitation after ring annuloplasty for ischemic mitral regurgitation. Ann Thorac Surg 2009;88:1197–1201. [PubMed: 19766807]

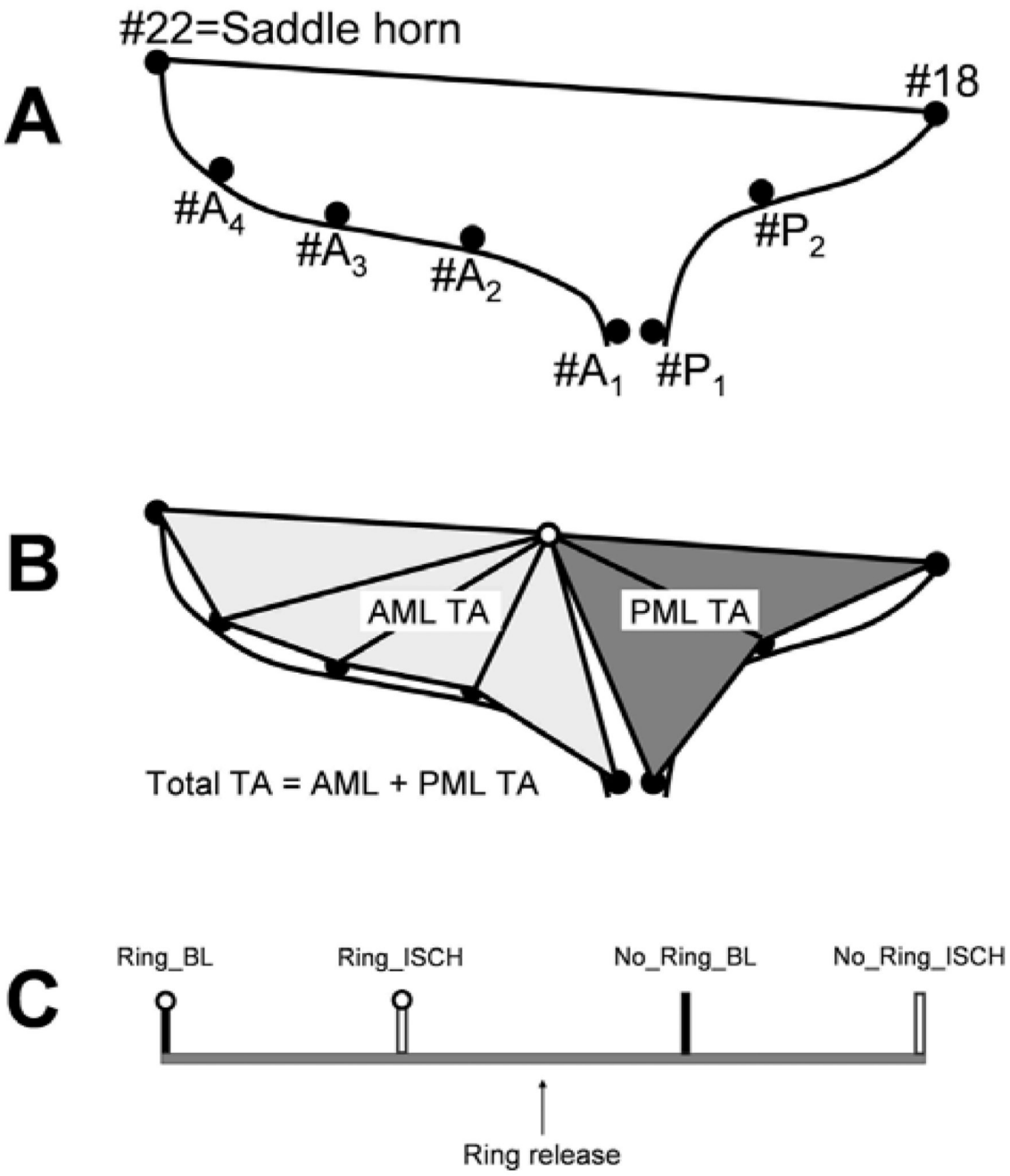

Figure 1.
Schematics depicting the **A**: marker array used to delineate the septal-lateral (S-L) aspects of the mitral annulus (#22 and 18), anterior mitral leaflet (AML, #A1–4) and posterior mitral leaflet (PML, #P1 and 2); **B**: calculation of AML and PML tenting areas; **C**: experimental protocol timeline (see METHODS for details).

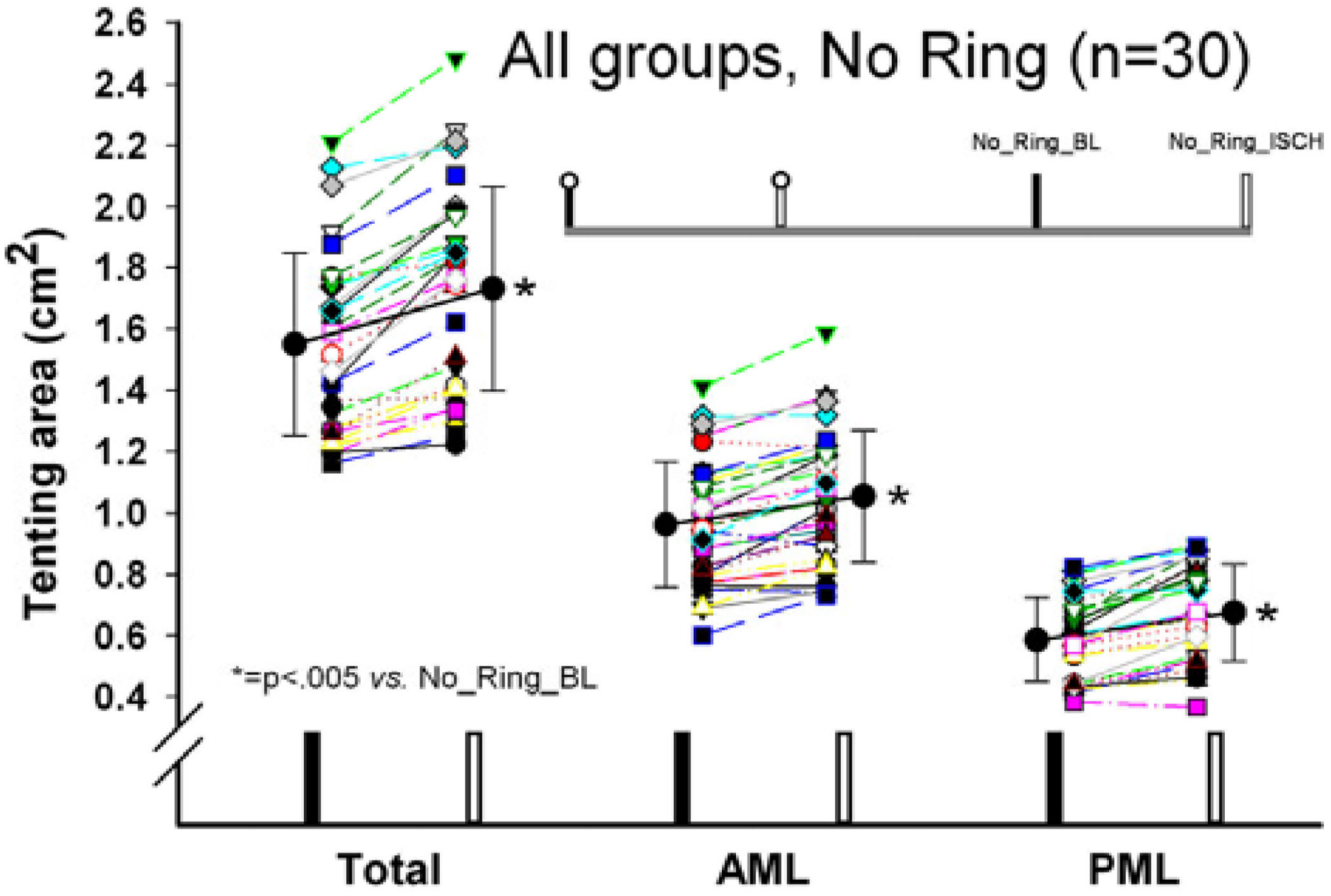

Figure 2.
Total, anterior and posterior mitral leaflet (AML and PML, respectively) septal-lateral (S-L) tenting areas in animals from all three groups with no ring implanted under baseline conditions and during acute postero-lateral LV ischemia.

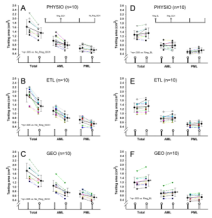

Figure 3.
Total, anterior and posterior mitral leaflet (AML and PML, respectively) septal-lateral (S-L) tenting areas in animals from all three groups during acute postero-lateral LV ischemia with and without annuloplasty ring (**A-C**) and with annuloplasty rings implanted under baseline conditions and during ischemia (**D-F**).

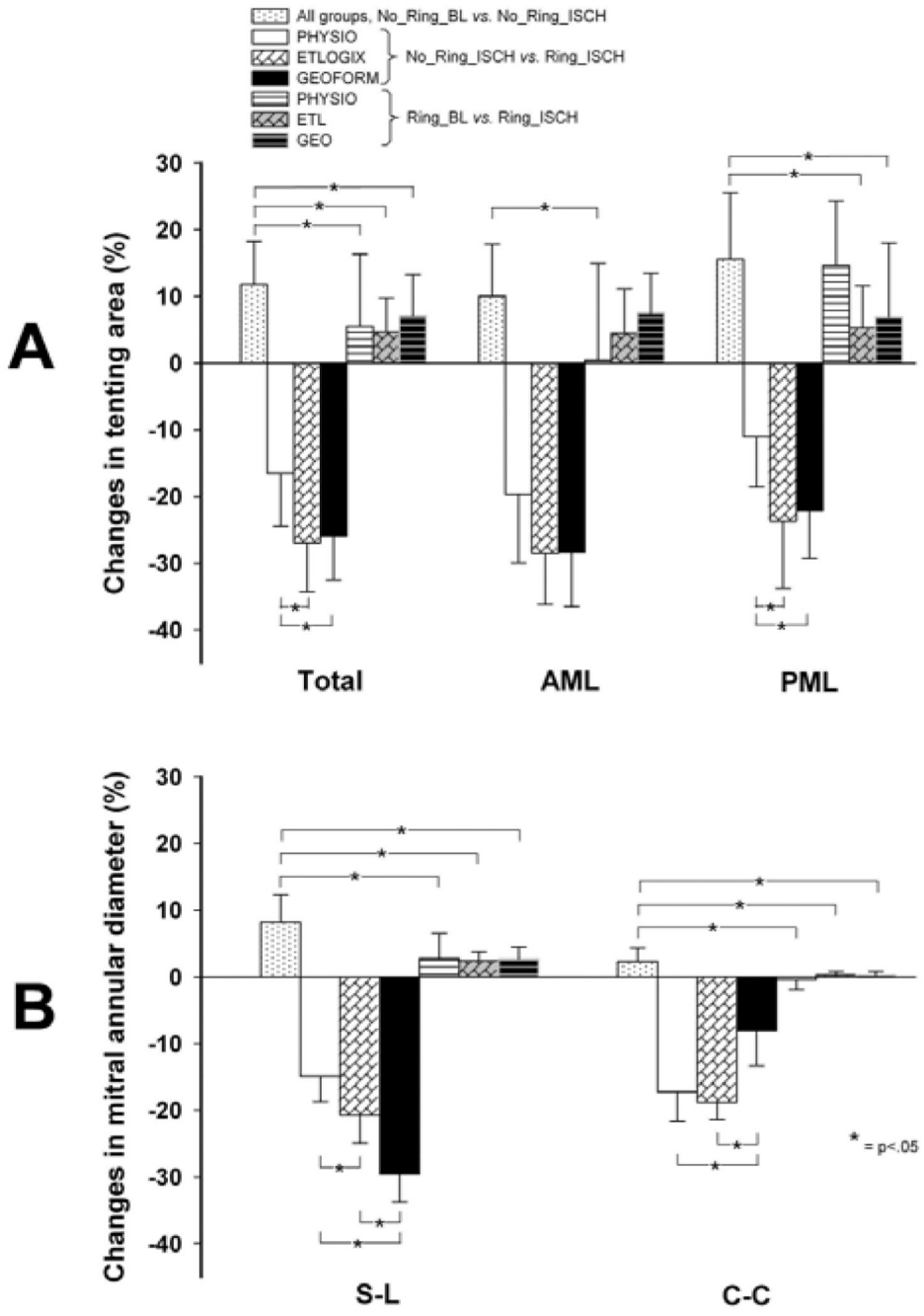

Figure 4.

Relative changes in tenting area (**A**) and mitral annular diameters (**B**) between the respective experimental conditions (see METHODS for details).

Table 1

Hemodynamic data and mitral annular dimensions

	PHYSIO				ETL				GEO			
	No_Ring_BL	**No_Ring_ISCH**	**Ring_BL**	**Ring_ISCH**	**No_Ring_BL**	**No_Ring_ISCH**	**Ring_BL**	**Ring_ISCH**	**No_Ring_BL**	**No_Ring_ISCH**	**Ring_BL**	**Ring_ISCH**
MR grade	0.6±0.2	1.1±0.4*	0.2±0.2	0.4±0.3	0.3±0.3	1.2±1.2*	0.2±0.2	0.2±0.2	0.5±0.4	1.5±0.9*	0.2±0.2	0.2±0.3
HR (min^{-1})	93±13	90±11	92±12	90±14	82±7	82±6	80±10	82±7	91±10	92±10	92±11	93±10
LVEDV (ml)	124±24	133±34*	124±26	135±36$^{\#}$	126±21	130±23	126±21	131±22$^{\#}$	112±14	122±17*	110±13	121±16$^{\#}$
dP/dt_{max} (mmHg/sec)	1324±330	1005±231*	1365±332	1077±225$^{\#}$	1177±387	921±294*	1201±380	923±239$^{\#}$	1342±335	1012±242*	1407±448	1085±231$^{\#}$
LVP_{max} (mmHg)	94±9	71±7*	94±6	75±9$^{\#}$	94±4	72±9*	96±4	75±7$^{\#}$	95±10	74±7*	96±6	76±6$^{\#}$
S-L (cm)	2.73±0.27	2.95±0.31*	2.44±0.16	2.50±0.16$^{\#}$	2.80±0.21	3.00±0.20*	2.32±0.15	2.38±0.15$^{\$\#}$	2.67±0.21	2.91±0.21*	1.99±0.09	2.04±0.09$^{\$\#}$
C-C (cm)	3.92±0.23	4.00±0.28*	3.31±0.07	3.30±0.08$^{\#}$	3.87±0.26	3.96±0.24*	3.20±0.15	3.21±0.16$^{\#}$	3.74±0.27	3.83±0.30*	3.50±0.11	3.51±0.11$^{\#}$

All data are mean±1 SD,

* p<.05 *vs.* No Ring BL,

$^{\$}$ p<.05 *vs.* Ring BL,

$^{\#}$ p<.05 *vs.* No Ring ISCH, MR, mitral regurgitation; HR, heart rate; LVEDV, left ventricular end-diastolic volume; LVP, left ventricular pressure; S-L, septal-lateral; C-C, commissure-commissure. ETL, IMR-ETLogix; GEO, GeoForm. ISCH, ischemia.